Manuscript Details

Manuscript number	YBENG_2017_969
Title	Drying rate control in microwave assisted processing of sliced apples
Article type	Research Paper

Abstract

The most enhanced systems perform microwave related drying of fruits and vegetables by continuously adjusting the power level in order to maintain the product temperature over a target value. As a result, typical drying curves are followed which exhibit fast drying rates in the middle stage. That can often lead to quality damage or undesirable changes in the food colour and texture. In response to these issues, a microwave system able to realize apples drying processes by keeping constant evaporation rates is proposed. This approach requires a continuous temperature adjustment of the apple slices under test, whose thermal level is detected by computer aided infrared thermography system. Since temperature corrections are required only during the middle stage of the process, the overall drying time is only slightly affected by the proposed control strategy. Nevertheless, compared to microwave drying with different constant temperatures: 60, 70 and 80°C, the resultant benefits operating at constant evaporation rates, include an improvement of texture and rehydration properties, while no differences in colour of sliced apples were observed.

Keywords	microwave; drying; infrared thermography; apple; color; texture
Manuscript region of origin	Europe

Corresponding Author	luciano cinquanta
Corresponding Author's Institution	University of Molise
Order of Authors	gennaro cuccurullo, Laura Giordano, Antonio Metallo, luciano cinquanta
Suggested reviewers	Reza Amiri Chayjan, S.N. Karaaslan

Submission Files Included in this PDF

File Name [File Type]

Highlights.docx [Highlights]

GraphAbs.docx [Graphical Abstract]

MW_Apple_2017.docx [Manuscript File]

Figure 1 - Schematic.tif [Figure]

Figure 2-Drying curves.tif [Figure]

Figure 3-Drying rate curves.tif [Figure]

Figure 4 - The fundamental mapping .tif [Figure]

Figure 5 - Constant temperature tests.tif [Figure]

Figure 6 - Control of the drying rate.tif [Figure]

Figure 7 - Maximum and average surface temperature evolution.tif [Figure]

Highlights

- A microwave system with constant evaporation rate was developed for apples drying.
- Constant evaporation rate operations helped to reduce product hotspots.
- Constant evaporation rate did not affect the color of microwaved dried apples
- Microwave drying with constant evaporation rates seems to improve apples texture

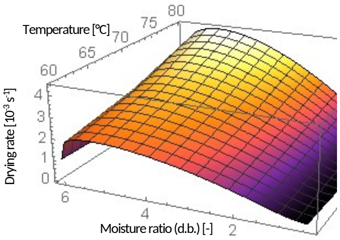
Temperature [°C]
60
65
70
75
80
Drying rate [10^{3} s^{-1}]
0
1
2
3
4
6
4
2
Moisture ratio (d.b.) [-]

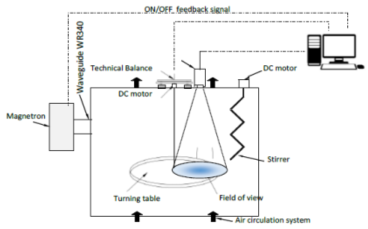
ON/OFF, feedback signal
Waveguide WR340
Technical Balance
DC motor
DC motor
Magnetron
Stirrer
Turning table
Field of view
Air circulation system

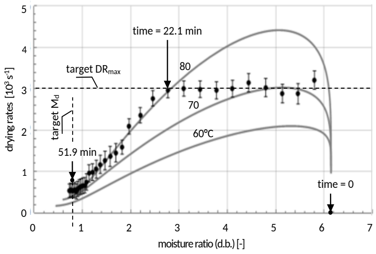
time = 22.1 min
80
70
60°C
target DR$_{max}$
target M$_{d}$
51.9 min
time = 0
drying rates [10^{3} s^{-1}]
moisture ratio (d.b.) [-]
0
1
2
3
4
5
6
7

Drying rate control in microwave assisted processing of sliced apples

Gennaro Cuccurullo [a], *Laura Giordano* [a], *Antonio Metallo* [a], *Luciano Cinquanta* [b,*]

[a] Dipartimento Ingegneria Industriale, University of Salerno, Italy

[b] Dipartimento Scienze Agrarie, Alimentari e Forestali, University of Palermo, Italy

*corresponding author. Luciano.Cinquanta@gmail.com

Key words: microwave; drying; infrared thermography; apple; color; texture

Abstract. The most enhanced systems perform microwave related drying of fruits and vegetables by continuously adjusting the power level in order to maintain the product temperature over a target value. As a result, typical drying curves are followed which exhibit fast drying rates in the middle stage. That can often lead to quality damage or undesirable changes in the food colour and texture. In response to these issues, a microwave system able to realize apples drying processes by keeping constant evaporation rates is proposed. This approach requires a continuous temperature adjustment of the apple slices under test, whose thermal level is detected by computer aided infrared thermography system. Since temperature corrections are required only during the middle stage of the process, the overall drying time is only slightly affected by the proposed control strategy. Nevertheless, compared to microwave drying with different constant temperatures: 60, 70 and 80°C, the resultant benefits operating at constant evaporation rates, include an improvement of texture and rehydration properties, while no differences in colour of sliced apples were observed.

Symbols and abbreviations

Symbol or abbreviation	Unit	Meaning
MW		microwave
IR		infrared
EM		electromagnetic
RMSE		root mean square error
d.b.		dry basis
i.d.		internal diameter
o.d.		outside diameter
$M_d(t)$	-	moisture content on dry basis
$m_{water}(t)$	kg	moisture content at time t
m_{dry}	kg	dry mass
$DR(t)$	s^{-1}	drying rate
DR_{max}	s^{-1}	target value of $dr(t)$
a	s^{-1}	equation fitting coefficient
b	s^{-c-1}	equation fitting coefficient
c	-	equation fitting coefficient
d	s^{-e}	equation fitting coefficient
e	-	equation fitting coefficient
$\Gamma(\beta,z) = \int_z^\infty t^{\beta-1} e^{-t} dt$		incomplete gamma function
T_{max}	[°C]	maximum surface temperature
t_{max}	s	time for which $M_d = 0.8$
NEB		non enzymatic browning
WI= $100 - \sqrt{(100-L^*)^2 + a^{*2} + b^{*2}}$		white index
L*		brightness
a*		red index
b*		yellow index

1. Introduction

Over the last decades, attractive results arising from microwave (MW) heating led to develop several techniques to control temperature level. It is well known that realizing MW assisted drying under appropriate processing conditions can increase speed of operation; improve fruit food quality, such as colour and texture, while reducing energy consumption (Gunasekaran, 1999). Researchers have studied various microwave power control profiles in order to meet consumer expectations by high quality food products, thus, intermittent methods and continuous methods have been proposed, most of them based on keeping power density or temperature under control (Zhenfeng, Wang, Raghavan & Cheng, 2006; Cuccurullo, Giordano, Metallo & Cinquanta, 2017).

Operating at constant power rates determines unuseful temperature increases in the early stage; meanwhile it causes undesirable changes in quality, such as browning of fruit surface colour and charring (Raghavan, Zhenfeng, Wang & Gariépy, 2010; Zhenfeng, Raghavan, Wang & Vigneaultd, 2011). According to Clark (1996) and Nijhuis et al. (1998), excessive temperatures along the edges and corners of products may lead to overheating and irreversible drying-out resulting in possible scorching and development of off-flavours.

Drying of fruit at constant temperature usually implies a typical drying curve is followed featured by rapid evaporation in the middle stage. In general, a complete MW drying is featured by three drying periods: I) heating-up period, in which the temperature of the product increases with time and the material starts to lose moisture at relatively small rates; II) middle stage drying period, during which a stable temperature profile is established and drying rates are highest; III) falling rate period, during which drying rates progressively slow down.

One of the major drawbacks of this control strategy is that too rapid mass transport by MW power may cause quality damage or undesirable changes in the food texture (Koné et al. 2013). Therefore, a suitable and adjustable temperature level or energy density should be set in order to encompass the opposite requirements: product quality, time and energy consumptions. In this framework, Raghavan et al. (2010) developed a microwave drying system, which allowed linearizing the drying curve in the middle stage; to this purpose, the power level was varied thus reducing product temperature, which was online recorded by a fibre optic sensor. Some researchers (Zhenfeng et al. 2006; Zhenfeng et al, 2011) presented an evolution of this system, which was based on a fuzzy logic control able to adjust the drying curves by monitoring volatiles emanating from carrots during drying.

In the present paper, a control system able to slow down the drying rate in the middle stage of the drying process is designed in order to keep the drying rate at a constant value. The developed system adjusted continuously the drying temperature depending on the actual moisture content and on the target temperature level of the apples slices under test. At this aim, an infrared camera looking at the surface samples temperatures was used to set the magnetron delivered power. Then, a relationship among temperature, drying rate and moisture content of the samples was established by suitable data processing based on a preliminary characterization of their drying kinetics. Five parameters fitting curve was introduced able to fairly adapt samples behaviour during all the stages of the drying process, whereas typical data fitting involves the falling rate period. The quality of the dried apples was assessed by colour and texture analysis, as well as rehydration capacity.

2. Materials and method

2.1 Microwave prototype

Drying experiments were carried out using a Lab scale MW plant (Figure 1), which houses a magnetron with a nominal power output of 2 kW operating @ frequency of 2.45 GHz. The reverberating chamber was a metallic cubic room (1m^3) equipped with a fan placed on the bottom of the cavity for continuous air renewal. Fresh air was introduced in the chamber at constant rate and temperature (25°C room temperature). A stirrer was placed inside the oven to improve heating uniformity (Cuccurullo et al., 2017; Zhenfeng, Raghavan & Wang, 2010). A Teflon rotating annulus (500 mm i.d., 550 mm o.d.) held a high-density polyethylene squared grid (10 mm x 10 mm), which supported the samples to be tested. The grid was connected to a technical balance (Gibertini EU-C 1200 RS, Novate Milanese, Italy) located on the top of the oven for online measuring moisture loss; the acquisition rate was 120 samples per minute.

An infrared (IR) thermometry system (ThermaCAM Flir P65, Canada) looked at the surface temperatures of the samples through a square hole (70 mm x 70 mm) realized on the oven top surface. The hole was properly shielded with a metallic grid, which allowed the IR radiation from the detected scene to escape but entrapping the microwaves (Li et al., 2010). A specifically realized LabView ® software was employed for acquiring the feedback signal produced every 0.9 s by the IR equipment. Then, the code allowed switching on-off the magnetron delivered power through an I/O board (AT MIO 16XE50, National Instruments, Assago, Italy). The actual temperature level was then adjusted according to the actual moisture ratio measurements, as shown in paragraph 2.3.

2.2 Samples preparation

Fresh apples (*Golden delicious*) were purchased from a local market and stored at 4°C before drying. Apples were cut into slices (10±0.2 mm thick, 20±0.3 mm diameter) using a sharp edged stainless steel pipe. The average initial moisture content of the samples was about 86 ± 0.7%, as resulted by heating samples in a convective oven with air at 105 °C, until a constant weight. Slices were placed on the support grid suspended in the MW oven

(Figure 1). The total applicator load was 200 g. All experimental tests were performed in triplicates.

2.3 Data acquisition and reduction

A suitably developed LabView 7.1 (National Instruments Corp., Austin, Texas) code was realized for both data acquisition/reduction and to control the magnetron delivered power. Data on exhaust air temperature and humidity, instantaneous sample weight were collected as well. Moreover, the code acquired the samples surface radiosity map as detected by the IR camera and converted it into temperature values. The camera was calibrated as previously reported (Cuccurullo, Giordano, Albanese, Cinquanta & Di Matteo, 2012). A number of samples, corresponding to about 30% of the total, were gathered in the IR scene every 0.9 s. Because of the turntable rotation, different random samples were detected when analysing different images.

Preliminary experimental tests were carried on by maintaining the surface temperature level of the samples under test at different target values, i.e. 60, 70 and 80 °C. The code, after extracting the maximum samples surface temperature from the IR images at time *t*, compared it to the corresponding set point to realize the required on/off operation. The end of the experimental tests was conventionally determined when the moisture content on dry basis

$$M_{\mathrm{d}}(t)=\frac{m_{water}(t)}{m_{dry}} \tag{1}$$

reached a residual value of 0.8, (Figure 2). The latter target value is selected such as the uncertainty related to samples actual weight (± 0.1 g) determines the end of the test with an error less than 30 seconds. Then, after performing a polynomial regression of the experimental data to smooth out short-term fluctuations, each two minutes the corresponding drying rates curves were calculated evaluating the analytical derivative

$$\mathrm{DR}(t)=\frac{1}{m_{dry}}\frac{\mathrm{d}m_{water}(t)}{\mathrm{d}t} \tag{2}$$

The experimental sets of (DR, t) were fitted by the empirical model

$$\mathrm{DR}(t)=a-b\,t^{c}\exp(-d\,t^{e}) \tag{3}$$

where the five constants *a*-*e* are equation-fitting coefficients, DR is expressed in s^{-1} and *t* in minutes. The mathematical structure of the previous equation allowed shaping the drying behaviour typically featuring MW drying during the whole process (Figure 3). In fact, it was observed (Maskan, 2000; Wang, Xiong & Yu, 2004; Chayjan & Alaei, 2013; Cuccurullo et al. 2017) that curves are featured by a short "warming up period" after which slowing down evaporating rates are progressively realized until a slope inversion takes place to smoothly recover the falling rate behaviour. The addressed trend is probably due to the different thermal history featuring each individual slice because of the uneven temperature field in the EM cavity. Unlike traditional drying, where empirical models work only in the falling rate period (Karaaslan & Tuncer, 2008), such a behaviour allows the proposed fit to be extended to the whole drying process: the fit satisfyingly recovers the experimental trend; the related coefficients and the Root Mean Square Error (RMSE) are reported in Table 1. Here, the times needed to complete the drying tests are reported as well.

The availability of eq. (3) allows retrieving coherently the fitting curve for the experimental sets (M_d, t); integrating the previous equation and imposing the initial condition, M_d (t=0) = 6.14 yielded:

$$\mathrm{M}_d(t) = a\,t - (b/d)\,c^{-\frac{1+e}{d}}\,\Gamma(k, c\,t^d) + (b/d)\,c^{-\frac{1+e}{d}}\,\Gamma(k,0) + M_{d0};\; k = \frac{1+e}{d} \qquad (3)$$

were Γ(a, z) is the incomplete gamma function. Since the measured moisture ratio decay appears smooth and regular, the related fitting seems to be satisfying, (Figure 3); the resulting RMSE for the M_d are given in Table 1. By eliminating the time variable from the two previous data set, the measured drying rates were written as function of the instantaneous moisture content for each of the three selected temperatures (DR, Md). A linear interpolation among the above curves was made to explicitly obtain the "fundamental mapping", that is maximum surface temperature, $T_{\max}$, as a function of M_d and DR: $T_{\max}$ = f(M_d, DR), (Figure 4).

The knowledge of the fundamental mapping allowed fixing a relationship between the maximum surface temperature and the moisture ratio in correspondence of a preselected target value for the DR. On such basis, the LabView code was able to adjust the temperature after on line measuring the actual weight i.e. the moisture ratio.

2.4 Chemical and physical analysis

Malic acid, citric acid, glucose and fructose were determined by enzymatic kits (Boehringer Mannheim, Germany), pH was measured with a glass-electrode pH-meter (Hanna Instruments). Total phenols were determined with Folin-Ciocalteu reagent at 760 nm

(Cinquanta, Albanese, Fratianni, La Fianza & Di Matteo, 2013). Colour was obtained through a colorimeter Minolta Chroma Meter II Reflectance CR-400 (Cuccurullo et al. 2012). Non-enzymatic browning was evaluated by the absorbance variation at 420 nm using Perkin Elmer, Lambda Bio 40 spectrophotometer. Texture of apple samples was measured by means of Texture Profile Analysis (Cuccurullo et al. 2017). Data were analysed by Bluehill 2 software package (Version 2.5, Instron Corporation, High Wycombe, UK). The rehydration of dried apple slices was carried out according to Atarés, Chiralt & González-Martínez (2009).

Statistical analysis

Chemical and physical analysis were performed in triplicate for all trials. Data reported are means and standard deviations calculated from three replicates. The analysis of variance (ANOVA) was applied to the data. The least significant differences were obtained using an LSD test ($P< 0.05$). Statistical analysis was performed using an SPSS version 13.0 for Windows (SPSS, Inc., Chicago, IL, USA).

3. Result and discussion

3.1. Preliminary experimental tests

The recorded maximum temperature during experimental tests at 60 °C, 70°C and 80°C, are shown in Figure 5. Higher temperatures required longer times meanwhile the corresponding energy consumptions were roughly the same, as deduced by summing up all the time intervals were the magnetron was turned on (data not reported). The higher the temperature level, the higher temperature fluctuations resulted, probably owing to the reduction in dielectric loss factor with temperature (Cuccurullo et al. 2012). Moreover, temperature fluctuations become larger toward the end of the process when power density increased due to mass reduction. The standard deviations related to 60, 70 and 80 °C temperatures levels turned out to be 1.2, 1.6 and 2.2 °C respectively; these values were significantly below those recorded in a previous search because of the adoption of a mode stirrer (Cuccurullo et al. 2017).

3.2 Drying rate control

The maximum drying rate was arbitrarily chosen to be $DR_{max} = 0.003\ s^{-1}$ aiming to reduce thermal stress in the middle drying phase. Then, the control system started to modulate the magnetron delivered power according to the fundamental mapping previously identified, i.e. suitably reducing the temperature level of the samples under test. The resulting drying rates are reported in Figure 6; the fitted drying-rate curves for the each preset temperature level are shown for reference, as well. The ability of the system to recover the target DR_{max} is witnessed by the maximum relative error which is lower than 6.7% and by the RMSE which turns out to be 9.9 10^{-5} s^{-1}.

Inspection of Figure 6 shows that adapting temperatures to reduce evaporation rates is effective within the first 22.1 minutes of the drying process, i.e. roughly after the middle stage completion: in fact, since the samples upper limit for temperature is fixed at 80°C, a time threshold is attained for which the maximum temperature remains unchanged at 80°C. Therefore, in the late stage of the drying process, evaporation rates slow down continuously following a path at constant temperature. The overall time needed to complete the test turns out to be 51.9 minutes, therefore the drying slows down with respect to the test @ 80°C (-24.7%), however it is faster than the test @ 70°C (+10.4%), which exhibits almost the same quality, as will be shown later. In Figure 7, the average and the maximum surface temperature evolution during drying process are reported. While progressively loosing water content, holding constant the selected DR_{max} requires monotonically increasing the surface temperature of the samples under test. The modulation of the maximum surface temperature is evident: it is required in the first 22.1 minutes of the process, to reduce the high evaporation rates realized by operating at constant temperature. Then, when the samples upper limit for temperature is attained, the 80°C-constant temperature path is followed. Meanwhile, the sample average surface temperatures slightly decrease with time increasing, since the diminishing water mass determines higher generation rates and, in turn, higher temperature spans.

3.3. Quality assessment

The proximate composition of fresh apples (Table 2) showed a relevant content in polyphenols: about 140 ppm, as enzymatic browning is a consequence of phenolic compounds' oxidation by polyphenol oxidase, which triggers the generation of dark pigments. The constant drying rate did not affect the color of dried apples, measured by white index (WI), respect to references at controlled temperatures (Table 3). However, the browning caused by non-enzymatic browning, showed a significant decrease by operating at constant drying rate (Table 3).Texture is another important quality attribute of food products, at higher temperature (80°C), dehydrated apples showed a significant firmness increase (Table 3). A correlation between hardening of the apple and reduced rehydration capacity (data not reported) was also found at 80°C. When the drying temperature is high, cell membranes rupture and release water into the extracellular space and therefore the transport of water to the outside occurs predominantly through the extracellular space (Halder, Dhall & Datta, 2011), causing a stiffening of the structure. On the other hand, the tests carried out at constant drying rate resulted in softer texture compared to the samples at 80°C.

4. Conclusions

By a preliminary data reduction, a fundamental map with a relationship among the three main variables involved in the microwave drying process: the temperature level, the drying rate and the moisture ratio, was developed. A real time drying control system by a computer aided thermography system allowed switching on-off the magnetron to set an automatic control to adapt temperature level of the target apple slices so to realize fixed evaporation rates in the middle stage-drying period. The overall time needed to complete the drying process turned out to be comprised between the ones related to 70 and 80°C fixed temperature operations, but closer to the latter, ensuring finer product quality. In fact, a softening in apple slices dried with fixed evaporation rates was obtained respect to those dried at 80°C.

5. References

Atarés, L., Chiralt A., & González-Martínez, C. (2009). Effect of the impregnated solute on air drying and rehydration of apple slices (cv. *Granny Smith*). *Journal of Food Engineering,* 91, 2, 305-310.

Chayjan, R. A., & Alaei, B. (2013). Characteristics of thin layer microwave drying of apricot. *Electronic Journal of Polish Agricultural Universities*, 16, 12.

Cinquanta, L., Albanese D., Fratianni A., La Fianza G., & Di Matteo M. (2013). Antioxidant activity and sensory attributes of tomatoes dehydrated by combination of microwave and convective heating. *Agro Food Industry Hi-Tech*, 24, 35-38.

Clark, D. E. (1996). Microwave processing of materials. *Annual Review of Materials Science*, 26, 299-331.

Cuccurullo, G., Giordano, L., Albanese, D., Cinquanta, L. & Di Matteo, M. (2012). Infrared thermography assisted control for apples microwave drying, *Journal of Food engineering*, 112, 319-325.

Cuccurullo, G., Giordano, L, Metallo, A. & Cinquanta, L. (2017). Influence of mode stirrer and air renewal on controlled microwave drying of sliced zucchini, *Biosystems engineering* 158, 95-101.

Gunasekaran, S. (1999). Pulsed microwave-vacuum drying of food materials. *Drying Technology*, 17(3), 395-412.

Halder, A. A., Dhall & Datta, A. K. (2011). Modeling transport in porous media with phase change: Applications to food processing. Journal of Heat Transfer, *Transactions of the American Society of Mechanical Engineers*. 133(3): 031010-1–031010-13.

Karaaslan, S. N., & Tuncer, I. K. (2008). Development of a drying model for combined microwave fan-assisted convection drying of spinach. *Biosystems Engineering*, 1, 44-52.

Koné, Y. K., Druon, C., Etienne, D., Gnimpieba, Z., Delmotte, M., Duquenoy, A. & Laguerre, J. C. (2013). Power density control in microwave assisted air drying to improve quality of food, *Journal of Food engineering*, 4, 750-757.

Maskan, M. (2000). Microwave/air and microwave finish drying of banana. *Journal of Food Engineering*, 44, 71-78.

Nijhuis, H. H., Torringa, H. M., Muresan, S., Yuksel, D., Leguijt, C., & Kloek, W. (1998). Approaches to improving the quality of dried fruit and vegetables. *Trends in Food Science and Technology*, 9, 13-20.

Raghavan, G. S. V., Zhenfeng, L., Wang, N. & Gariépy, Y. (2010). Control of Microwave Drying Process Through Aroma Monitoring, *Drying Technology*, 28, 5, 591-599.

Wang, J., Xiong, Y.-S., & Yu, Y. (2004). Microwave drying characteristics of potato and the effect of different microwave powers on the dried quality of potato. *European Food Research Technology*, 219, 500-506.

Zhenfeng, L., Wang, N., Raghavan, G. S. V. & Cheng W. (2006). A microcontroller-based, feedback power control system for microwave drying processes, *Applied engineering in Agriculture,* 22, 309-314.

Zhenfeng, L., Raghavan, G. S. V. & Wang, N. (2010). Carrot volatiles monitoring and control in microwave drying, LWT - Food Science and Technology, 43 291-297.

Zhenfeng, L., Raghavan, G. S. V., Wang, N. & Vigneault, C. (2011). Drying rate control in the middle stage of microwave drying, *Journal of Food engineering*, 2, 234–238.

Figures captions

Figure 1. Schematic diagram of the microwave lab plant drying system.

Figure 2. Drying curves of apple slices during microwave heating at 60, 70 and 80 °C.

Figure 3. Drying rate curves during microwave drying of apples slices at 60, 70 and 80°C.

Figure 4. The fundamental mapping: linear interpolation among the maximum surface temperature ($T_{\max}$) of apples slices during microwave drying, as a function of moisture content on dry basis (M_d) and drying rate (DR).

Figure 5. Temperature fluctuations upon apple slices detected by infrared thermography during microwave heating at constant temperature (60, 70 and 80 °C).

Figure 6. Drying rates (DR) of apple slices as a function of moisture content on dry basis (M_d) during controlled drying rate tests (●). The vertical bars indicate the standard deviation.

Figure 7. Maximum and average surface temperature evolution upon apple slices during a controlled drying rate test

Table 1. List of the fitting parameters used in this work and related fit quality. RSME (root mean square error); DR (drying rate), M_d (moisture content on dry basis).

Tempe-rature [°C]	a	-b	c	d	e	Drying time [min]	RMSE DR [s^{-1}]	M_d [-]
60	$1.62\ 10^{-04}$	$1.71\ 10^{-03}$	$2.53\ 10^{-03}$	1.64	$9.76\ 10^{-02}$	80.1±4.3	$6.4\ 10^{-5}$	$4.67\ 10^{-2}$
70	$2.16\ 10^{-04}$	$2.33\ 10^{-03}$	$6.19\ 10^{-03}$	1.57	$1.62\ 10^{-01}$	57.9±2.3	$8.6\ 10^{-5}$	$8.63\ 10^{-2}$
80	$3.83\ 10^{-04}$	$3.16\ 10^{-03}$	$1.51\ 10^{-02}$	1.54	$2.68\ 10^{-01}$	41.6±3.3	$13.3\ 10^{-5}$	$5.04\ 10^{-2}$
variable						51.9±3.6	$9.9\ 10^{-5}$	

Table 2. Proximate composition (%) of fresh apples

Water	85.6 ± 0.7
Sugar	12.4± 0.3
pH	4.1± 0.1
Phenols*	140.2± 8.2
Citric acid	0.12± 0.02
Malic Acid	0.18± 0.03

*ppm of catechin

Table 3 - White index (WI), non-enzymatic browning (NEB) and hardness (N) in fresh and apples dried at different temperatures (60, 70 and 80*C) and at constant evaporation rate (CER).

Parameter	Fresh samples	Dried samples			
		60°C	70°C	80°C	CER
WI	69.2 ^{a}	46,9 ^{b}	48.9 ^{b}	50.7 ^{b}	48.5 ^{b}
NEB	0.05 ^{a}	0.28 ^{b}	0.30 ^{b}	0.26 ^{b}	0.21 ^{c}
Hardness	0.5^{a}	2.8 ^{b}	2.5 ^{b}	3.5 ^{c}	2.7 ^{b}

Unequal letter within same row indicate significative differences ($P < 0.05$) (standard deviation are not reported because below 5%)

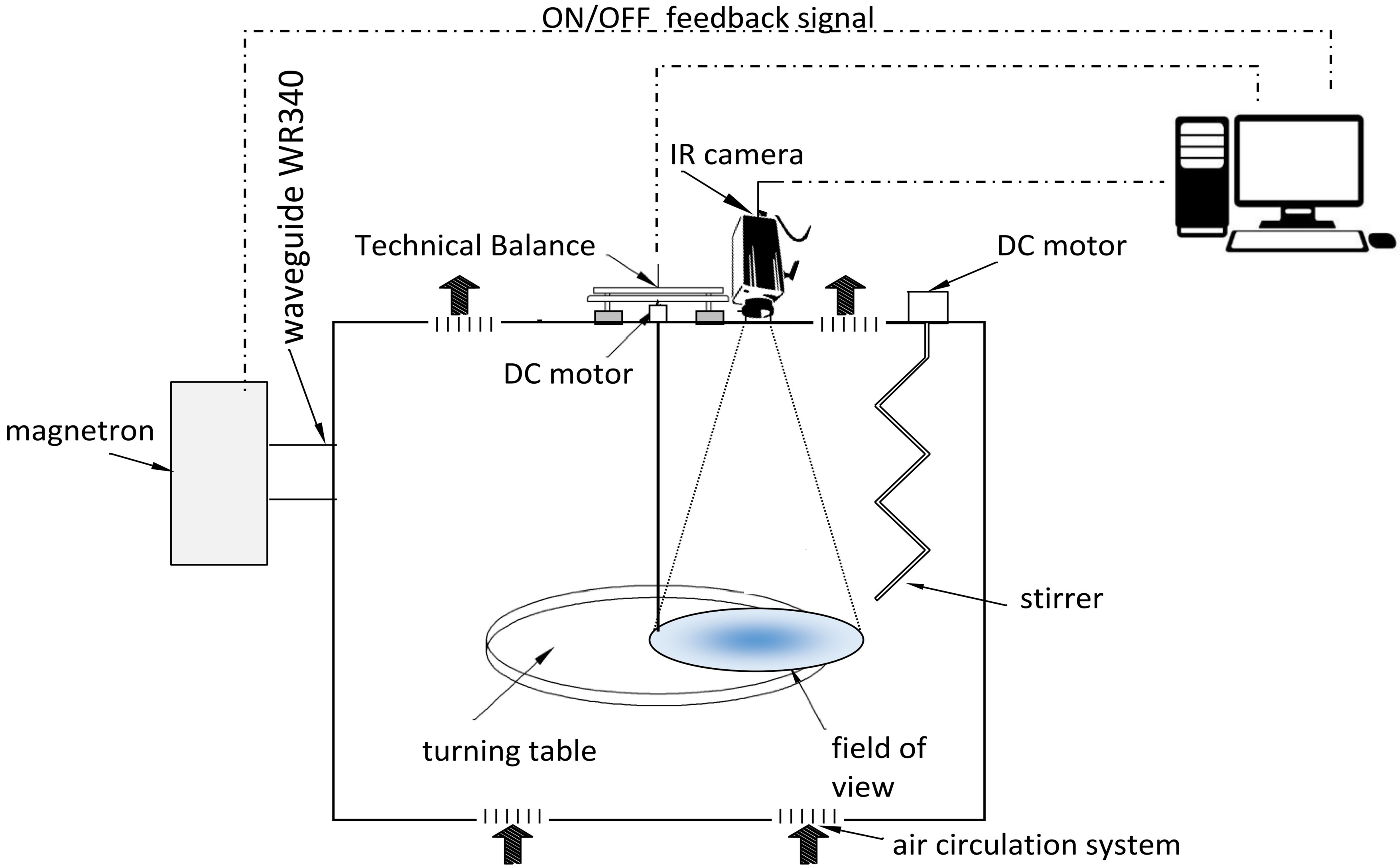
ON/OFF feedback signal
waveguide WR340
IR camera
Technical Balance
DC motor
DC motor
magnetron
stirrer
turning table
field of view
air circulation system

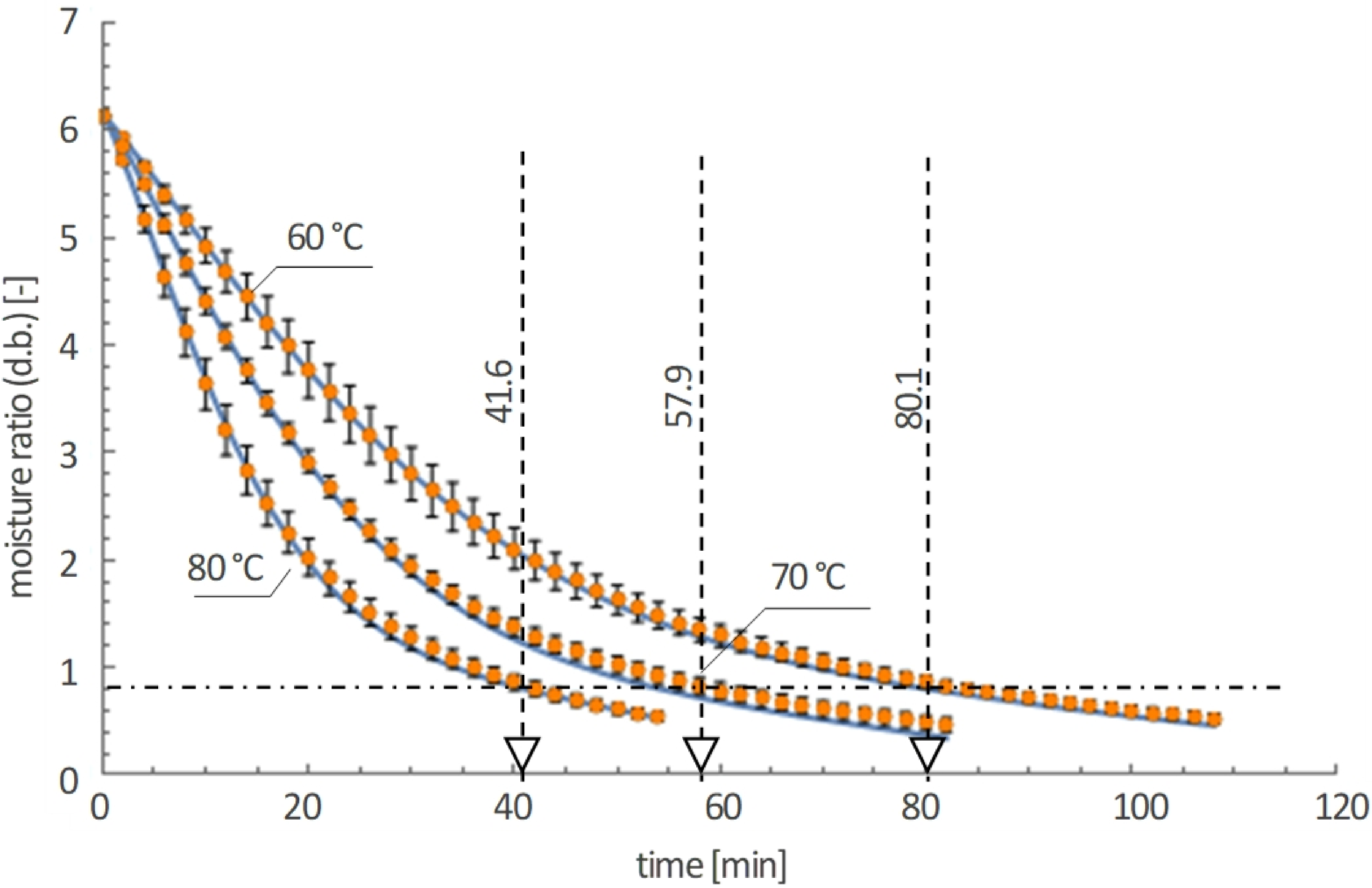

moisture ratio (d.b.) [-]
time [min]
60 °C
70 °C
80 °C
41.6
57.9
80.1
0
1
2
3
4
5
6
7
0
20
40
60
80
100
120

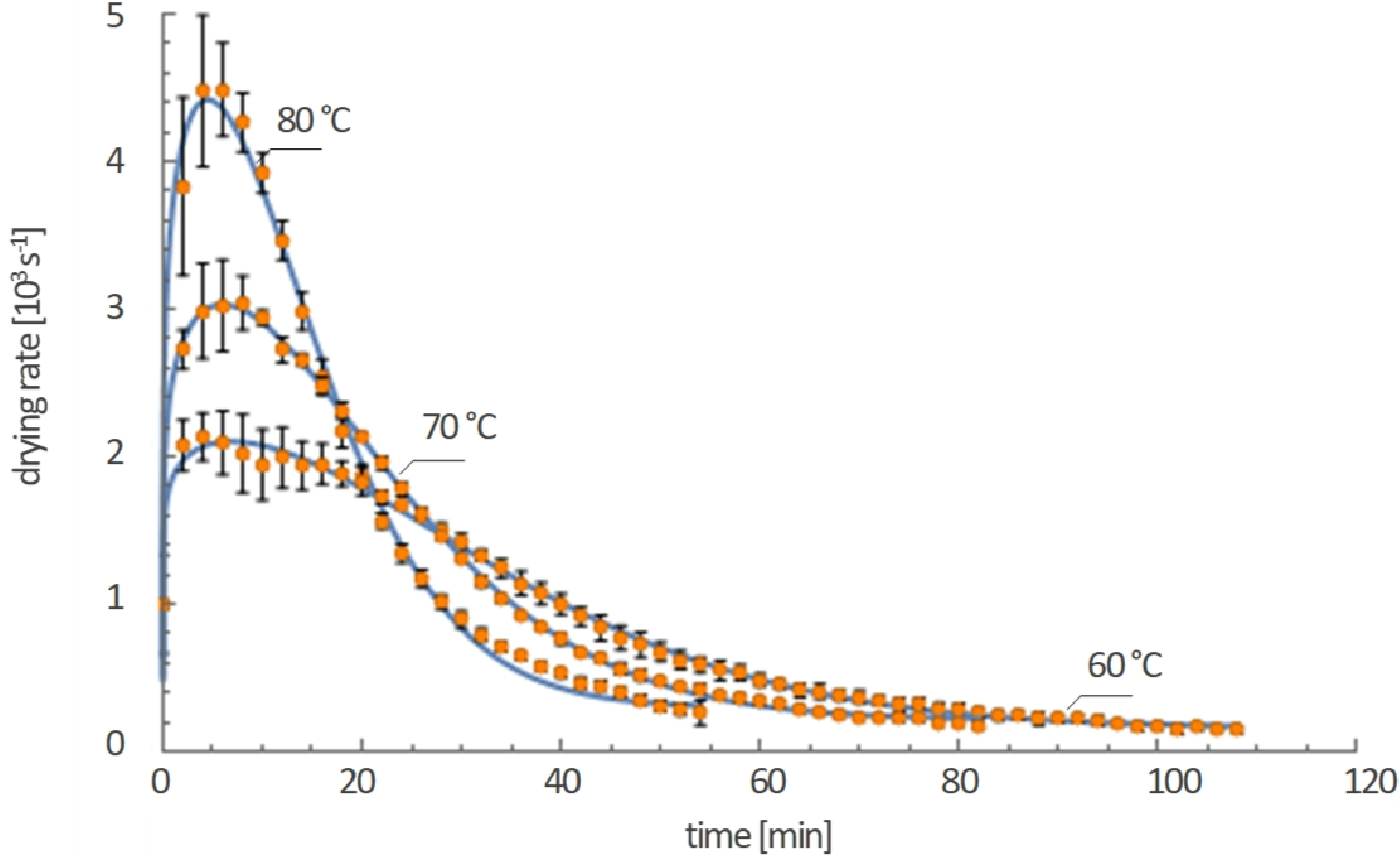

drying rate [10^3 s^{-1}]
time [min]
80 ℃
70 ℃
60 ℃
0
1
2
3
4
5
0
20
40
60
80
100
120

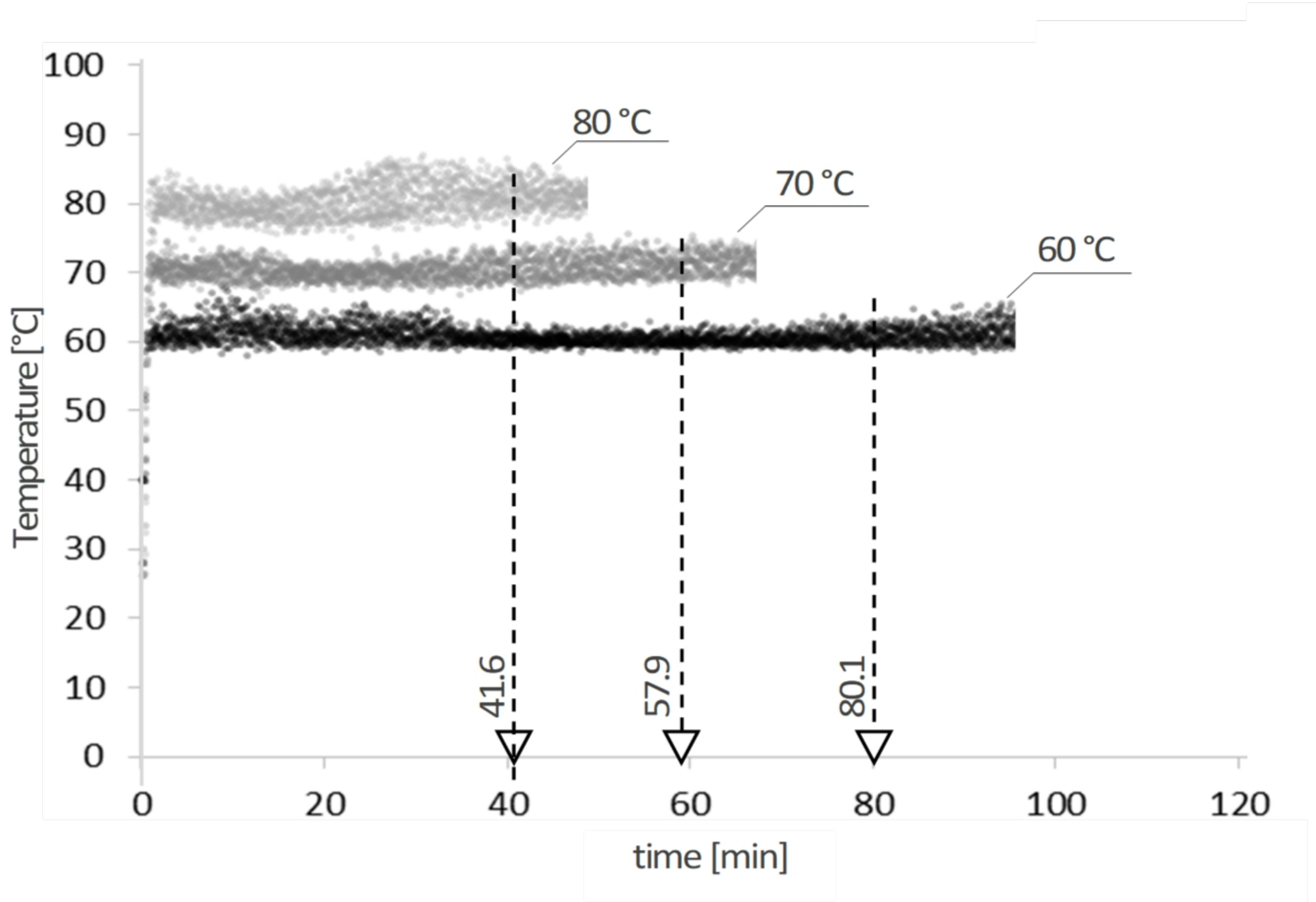

Temperature [°C]
100
90
80
70
60
50
40
30
20
10
0
80 °C
70 °C
60 °C
41.6
57.9
80.1
0
20
40
60
80
100
120
time [min]

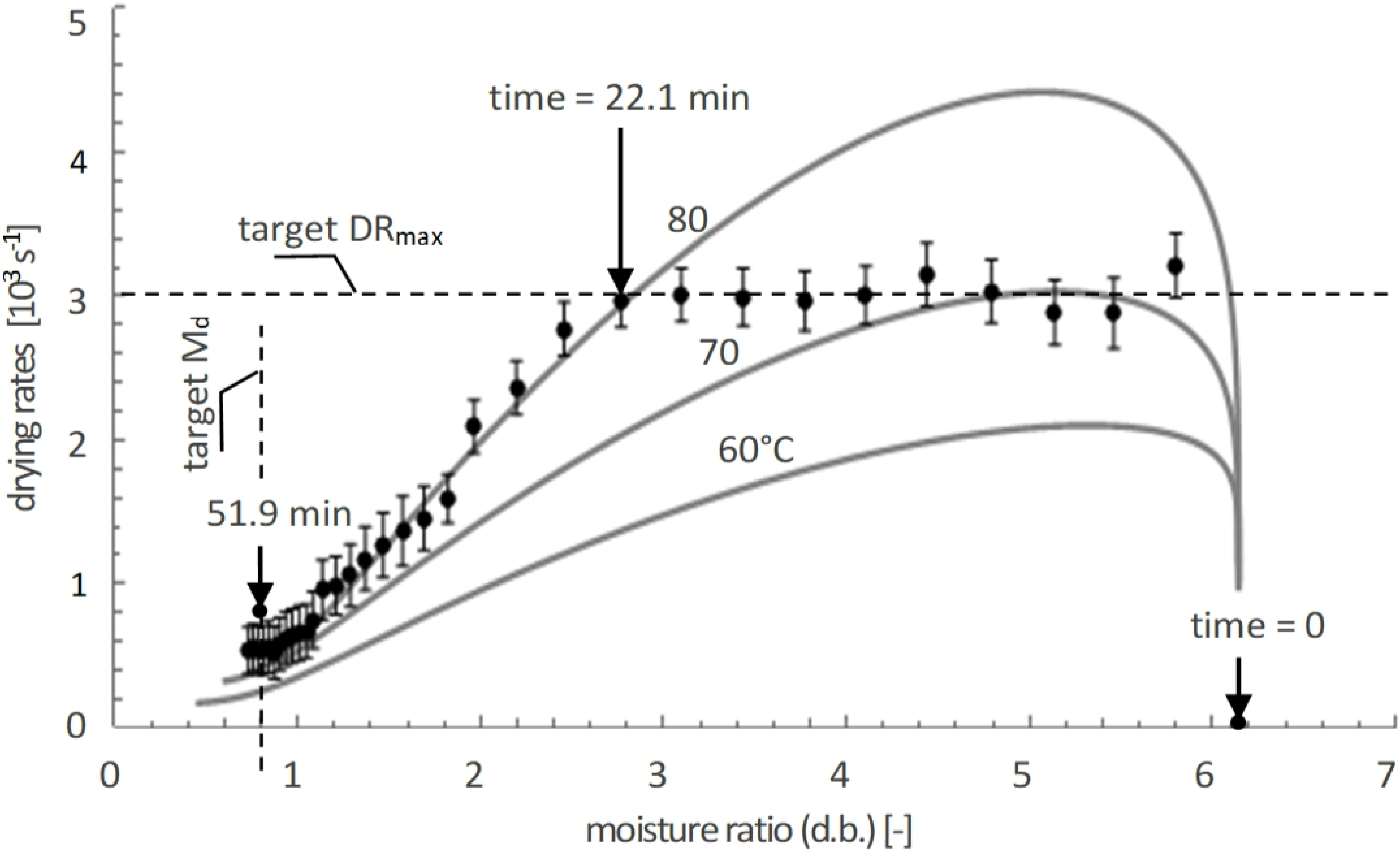

time = 22.1 min
target DRmax
80
70
60°C
target Md
51.9 min
time = 0
drying rates [10^3 s^-1]
moisture ratio (d.b.) [-]
0
1
2
3
4
5
6
7

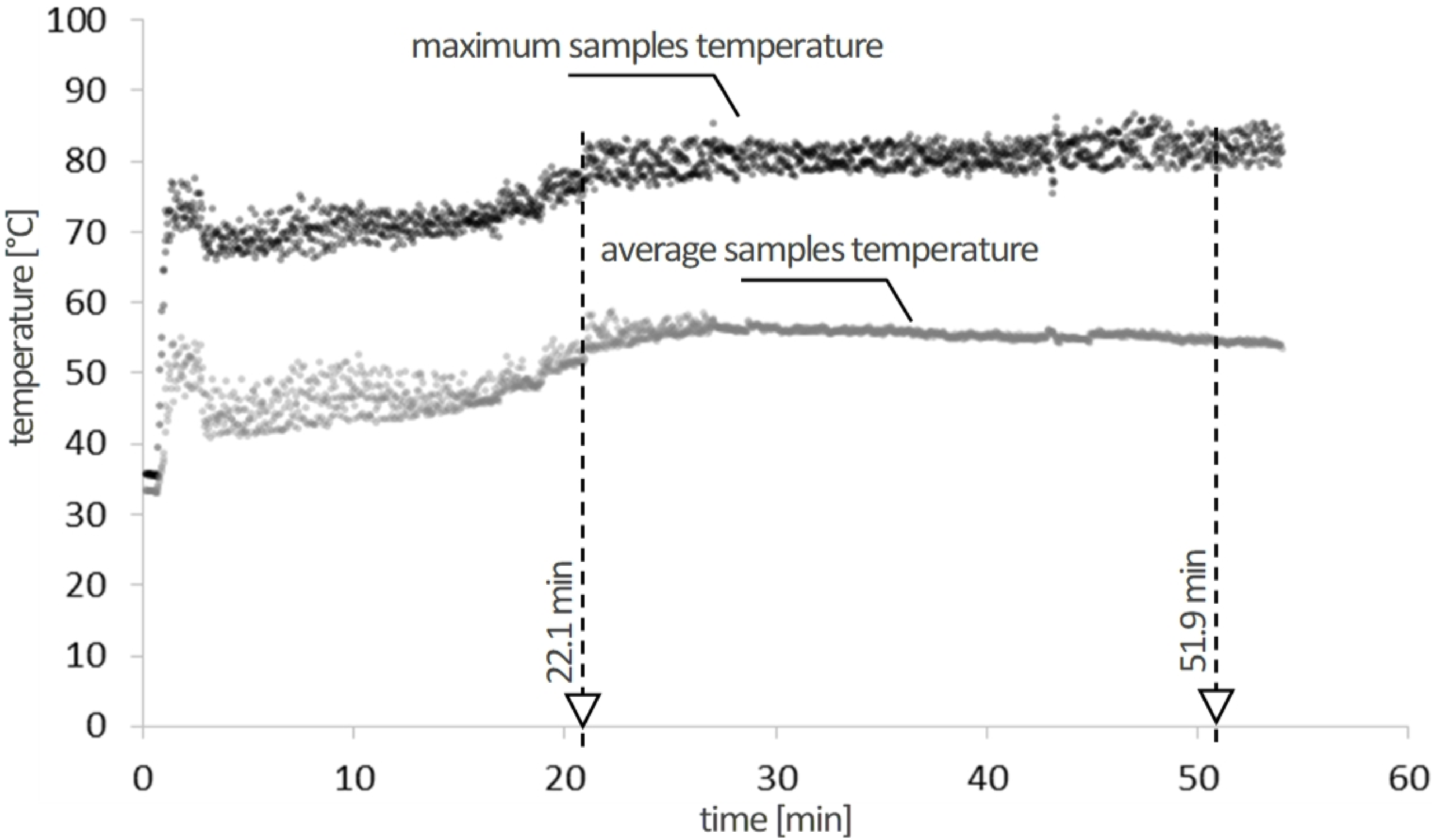

maximum samples temperature
average samples temperature
temperature [°C]
time [min]
22.1 min
51.9 min
0
10
20
30
40
50
60
70
80
90
100
0
10
20
30
40
50
60